Proceedings of the 21st ICSMGE, Vienna, Austria, 14 – 19 June 2026. Pistrol, Adam & Schweiger (eds.)
Published by: ÖGG, Austrian Society for Geomechanics, Salzburg, Austria, ISBN 978-3-9503898-4-5
https://doi.org/10.53243/ICSMGE2026-943

Impact of non-uniform temperature distributions on the stress behavior of energy walls: A numerical study

Mert Guner, Ugur Can Erginag, Ozer Cinicioglu
Department of Civil Engineering, Bogazici University, Turkey, mert.guner@bogazici.edu.tr

Semra Polat
School of Engineering, The University of Edinburgh, United Kingdom

Melis Sutman
Institute for Infrastructure and Environment, School of Engineering, University of Edinburgh, United Kingdom

ABSTRACT: Energy geostructures at shallow depths, such as energy piles, slabs, and walls, have gained prominence in geotechnical engineering as a means to reduce reliance on fossil fuels for heating and cooling. These systems serve a dual function, combining structural support with ground-source heat exchange. Among them, energy walls stand out due to their distinctive geometry and boundary conditions, which influence the development of thermally induced stresses. This study focuses on the axial stress distributions that arise in energy walls under non-uniform temperature fields, representative of realistic thermal loading during energy operations. A three-dimensional numerical model was developed in COMSOL Multiphysics to simulate both short- and long-term thermal scenarios. The results reveal that non-uniform axial temperature gradients lead to the simultaneous occurrence of tensile and compressive stresses along the wall height, with some tensile zones approaching or exceeding the concrete's allowable capacity. These insights emphasize the importance of accounting for thermally induced axial stress variations when evaluating the long-term structural performance of energy walls.

KEYWORDS: Energy walls, Thermal stresses, Non-uniform temperature distribution, Numerical modelling.

1 INTRODUCTION

Energy geostructures have emerged as effective solutions for integrating structural support with low-carbon heating and cooling systems (Brandl, 2006; Laloui and Sutman, 2021). Among these systems, energy piles have been extensively studied, particularly with respect to the thermal loads that develop during operation. Numerous studies have demonstrated that non-uniform temperature distributions across the pile cross-section can induce differential axial strains and complex stress patterns, including the simultaneous development of tensile and compressive stresses (Abdelaziz and Ozudogru, 2016; Faizal et al., 2019; Polat et al., 2025a, b; Erginag et al., 2025a, b). These findings have highlighted the importance of considering multi-dimensional thermal effects rather than assuming simplified uniform fields.

Although energy walls are subjected to thermal cycles similar to those observed in energy piles, their thermo-mechanical behavior has been studied far less extensively. In practice, the temperature increase within energy walls during heat exchange is not spatially uniform. The most significant rise typically occurs in the immediate vicinity of the heat exchanger pipes, while other regions of the structure experience substantially lower thermal changes. This leads to non-uniform temperature distributions along horizontal directions of the wall. Such gradients are further influenced by the wall's geometry, material properties, and boundary conditions including surface exposure, insulation layers, and contact with the surrounding ground. As a result, differential thermal expansion occurs, giving rise to axial tensile and compressive stresses that may compromise the structural integrity of the wall if not properly accounted for in design.

In this study, a detailed three-dimensional finite element model was developed using COMSOL Multiphysics to investigate the development of axial thermal stresses in energy walls under realistic operational conditions. To ensure the reliability of the numerical approach, the model was validated against experimental data reported by Xia et al. (2012). Following validation, the model was applied to simulate both summer and winter scenarios, representing short- and long-term heating and cooling cycles. These simulations allowed for an in-depth evaluation of time-dependent stress distributions resulting from non-uniform temperature gradients, offering valuable insight into the thermal behavior of energy walls under seasonal operation.

2 VALIDATION OF THE NUMERICAL MODEL

To evaluate the reliability of the developed numerical model, validation was performed using experimental data from Xia et al. (2012), which investigated the thermal performance of a diaphragm wall beneath the Shanghai Natural History Museum. In that study, the energy wall included U-shaped polyethylene (PE-100) heat exchanger pipes, each with an outer diameter of 25 mm and a wall thickness of 2.3 mm, installed at regular 75 cm intervals. These pipes were embedded within a 1 m thick C30 concrete diaphragm wall that extended to a total depth of 38 meters, with an excavation depth of 18.5 meters. The surrounding ground consisted mostly of Shanghai clay, which was fully saturated with no groundwater flow.

The selected test scenario involved continuous system operation for 48 hours, during which the heat carrier fluid entered the system at 35°C and a flow velocity of 0.6 m/s. Some geometric details, such as the full wall width, concrete cover thickness, and embedded pipe lengths, were not explicitly reported in the original study. To complete the numerical model, values were adopted from relevant literature: the wall width was taken as 1.5 m, the concrete cover as 100 mm, and the embedded pipe length as 37.5 m (Sun et al., 2013; Sailer, 2020; Bodas Freitas et al., 2024).

Initial temperature measurements from the field showed significant variation with depth, ranging from 12.2°C near the surface to 25.0°C at mid-depth and 21.2°C at the bottom. To reflect this stratification, the wall was divided into two thermal zones in the model: 23°C for the lower section and 16.3°C for the upper section. For consistency, the initial soil temperature was also set to 23°C. Adiabatic conditions were applied to the

lateral and bottom boundaries, while constant temperature (16.3°C) was assigned to exposed faces.

The thermal and mechanical properties of concrete and soil used in the numerical model are listed in Table 1.

Table 1. Material properties for soil and concrete.

Description	Symbol	Unit	Concrete	Soil
Density	ρ	kg/m^3	2500	1800
Thermal conductivity	λ	W/mK	1.6	1.74
Specific heat capacity	c	J/kgK	1046	1690
Thermal expansion coefficient	α	1/C°	12x10^{-6}	6x10^{-6}
Young's modulus	E	MPa	30000	23.7
Poisson's ratio	ν	-	0.2	0.33

2.1 *Comparison with experimental results*

To assess the accuracy of the numerical model, simulation results were compared with the experimental temperature data reported by Xia et al. (2012) for the 48-hour continuous operation test. As shown in Figure 1, the simulated temperatures closely matched the measured values, indicating that the model effectively captures the thermal behavior of the energy wall. A quantitative comparison revealed an average error of 6.2% during the initial 10 hours, which is reasonable considering the rapid temperature changes in the early phase. Between hours 10 and 48, as the temperature distribution became more stable, the average error decreased to 2.5%. Over the full test duration, the overall mean error was calculated as 3.3%, confirming the model's reliability in reproducing the measured thermal response throughout the simulation period.

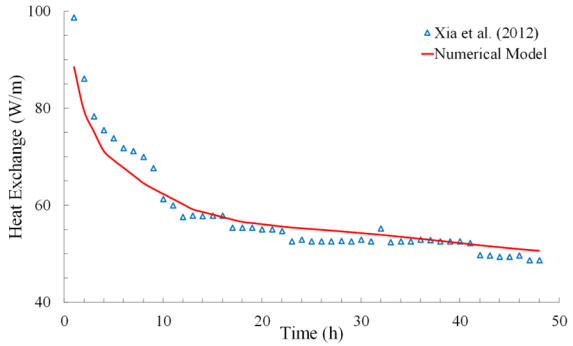

Figure 1. Comparison of measured data with numerical simulation.

3 NUMERICAL MODEL

The validated three-dimensional numerical model was employed to analyze the thermo-mechanical response of an energy wall under thermal loading. The model focused on the development of thermally induced stresses resulting from non-uniform temperature distributions during heating and cooling scenarios.

The simulation domain represents a diaphragm wall embedded in homogeneous soil, with total dimensions of 60 meters in height, 50 meters in width, and 3 meters in thickness. Two structural slabs, each 1 meter thick, were included to represent the ground-level and excavated-side support conditions. Heat exchanger pipes were modeled as line elements spaced at 0.75 meters and defined through the Heat Transfer in Pipes interface. The overall geometry, mesh configuration, and boundary conditions are shown in Figure 2.

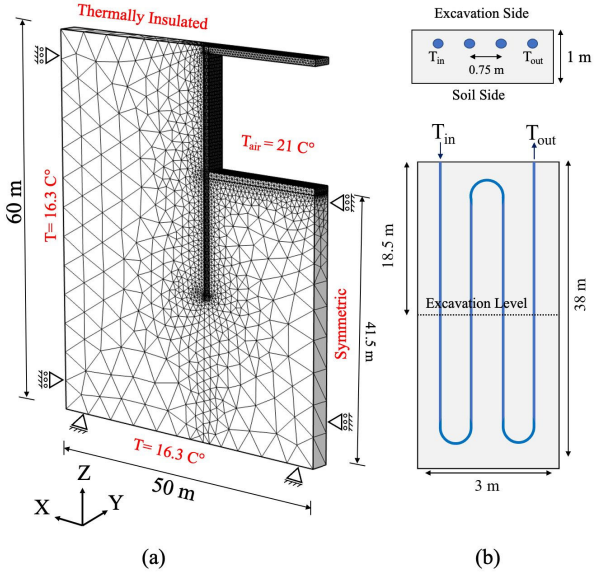

Figure 2. Numerical model setup: (a) 3D representation and boundary conditions and mesh configuration of the energy wall, (b) Cross-sectional layout of the pipe arrangement inside the energy wall.

The model includes three physics interfaces: Heat Transfer in Porous Media (for the wall and soil), Heat Transfer in Pipes (for the circulating fluid), and Solid Mechanics (for structural response). Thermal expansion was used to couple thermal and mechanical behaviors.

All materials were assumed to be isotropic, linear elastic, and fully bonded. Mechanical boundary conditions included fixed support at the base and roller constraints at vertical sides. For thermal boundary conditions, the entire model domain was initially set to a uniform temperature of 16.3°C. Constant temperature boundaries were also assigned as 16.3°C on the left and bottom surfaces. The right-side boundary was modeled as thermally symmetric (zero heat flux). Natural convection was applied to the exposed excavation surfaces, with an ambient air temperature of 21°C.

Two thermal loading cases were simulated: heating at 45°C and cooling at 5°C, both applied over 30 days. Material properties used in the model are summarized in Table 1.

4 RESULTS AND DISCUSSION

The results are presented with a focus on the axial thermal stresses that develop within the energy wall due to non-uniform temperature distributions. The evaluation is carried out on a representative cross-section located at a depth of 9 meters. This section was selected because it corresponds to the mid-depth of the part of the wall where one side faces the open environment and the other side is in direct contact with soil. This location corresponds to Section A, as illustrated in Figure 3. Axial (Z-direction) stresses were computed for both heating (summer) and cooling (winter) scenarios, and analyzed at four selected time intervals: 2 hours, 1 day, 7 days, 30 days. These results provide insight into the evolution of axial stress over time under realistic operational conditions.

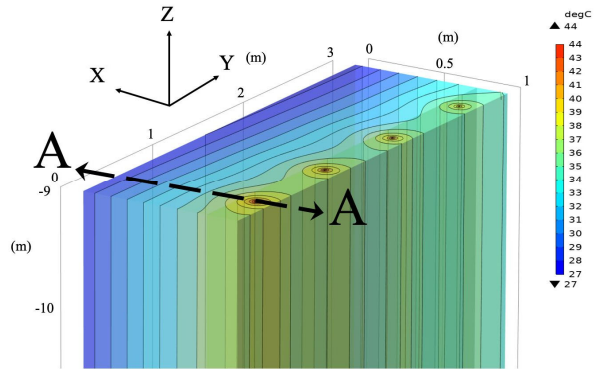

Figure 3. The locations of cross-section A taken from the energy wall.

4.1 *Formation of non-uniform temperature distribution*

Figures 4 and 5 show the non-uniform temperature distributions across the energy wall cross-section at a depth of 9 meters under heat injection and extraction scenarios. These results, visualized at four different time intervals, demonstrate how thermal gradients evolve with time. Additional profiles along Sections A are presented in Figures 6 and 7, allowing a more detailed examination of directional heat propagation.

At early time step (2 h), temperature changes are concentrated around the embedded pipes, forming circular thermal zones. This localized distribution results from the short time available for heat to diffuse through the wall mass. As time progresses, especially after Day 1, the heated or cooled region expands toward the building-facing side, and a secondary, more linear temperature gradient begins to develop.

This transition is clearly visible along Section A. While the circular temperature pattern around the pipes remains similar in shape, its intensity gradually decreases over time as the local temperature differences diminish. In contrast, a linear gradient near the building-facing side becomes increasingly pronounced, indicating progressive heat transfer through the wall thickness. Overall, the temperature in both regions continues to rise under heat injection or decrease under heat extraction.

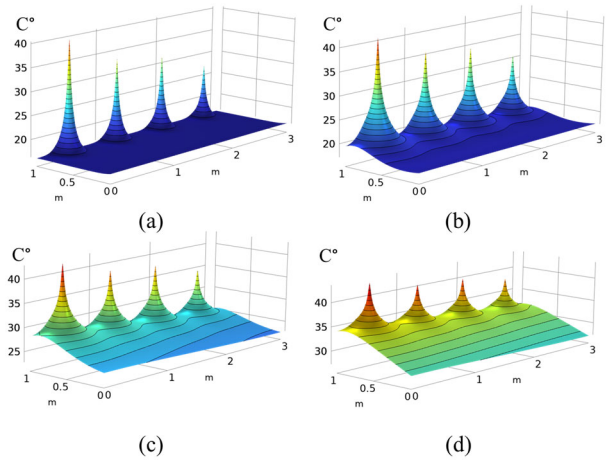

Figure 4. Evolution of non-uniform temperature distribution under the summer scenario at the 9-meter cross-section: (a) 2 h, (b) 1 day, (c) 7 days, (d) 30 days.

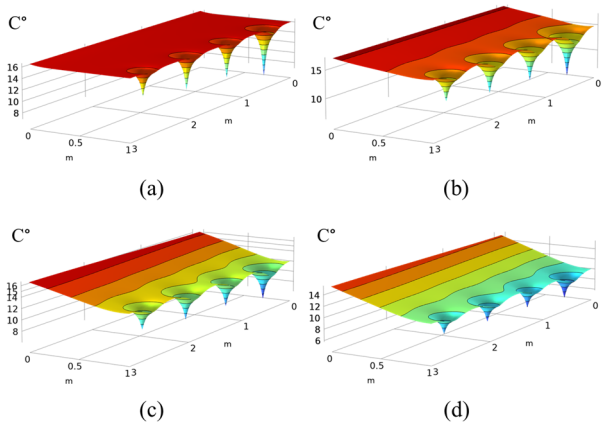

Figure 5. Evolution of non-uniform temperature distribution under the winter scenario at the 9-meter cross-section: (a) 2 h, (b) 1 day, (c) 7 days, (d) 30 days.

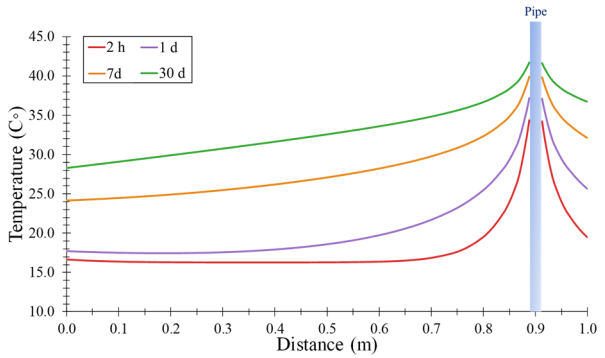

Figure 6. Distribution of temperature at section A for summer scenario.

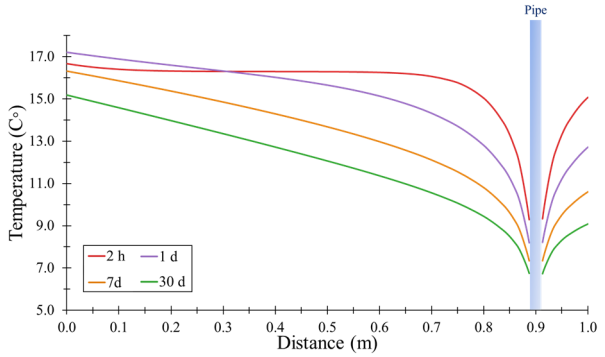

Figure 7. Distribution of temperature at section A for winter scenario.

4.2 *Axial thermally induced stresses*

Axial thermally induced stresses along Section A are presented in Figures 8 and 9 for the summer and winter scenarios, respectively. The spatial and temporal evolution of these stresses reflects the influence of non-uniform temperature distributions within the energy wall. In this study, positive values denote tensile stresses, while negative values correspond to compressive stresses.

In regions close to the embedded thermal pipes, where circular temperature gradients are most pronounced, the summer scenario leads to a rapid buildup of compressive axial stresses. These stresses peak within the early hours, reaching approximately 8 MPa at 2 hours, and then gradually decrease to around 4.45 MPa by day 90. This trend corresponds to the initial rapid heat gain near the pipes, followed by a gradual reduction in thermal gradient over time. In contrast, the winter scenario results in moderate tensile stresses in the same region, reaching

about 3.3 MPa at 2 hours, and slightly declining to 2.5 MPa by the end of the simulation period.

At the outer boundary of the wall, representing the edge of the circular temperature distribution and the interface between the concrete and surrounding soil, thermally induced stresses reach approximately 1.85 MPa by day 30 during the summer scenario. Under winter conditions, compressive stresses reach around 1.25 MPa.

Near the building-facing surface of the wall, corresponding to the region influenced by a more linear temperature distribution, thermal stresses follow a different trend. In the summer case, compressive stresses near the pipes transition into tension toward the building-facing side. Conversely, in the winter case, tensile stresses near the pipes turn into compression closer to the building-facing side. By day 30, these stresses reach approximately 1.85 MPa in tension (summer) and 1.25 MPa in compression (winter). This behavior illustrates the directional propagation of heat through the wall thickness and its role in shaping axial stress distributions.

Overall, the results demonstrate that spatially varying temperature fields, originating from the geometry and placement of heat exchanger pipes, create complex internal stress patterns, which evolve with time and influence the structural performance of energy walls under seasonal operation.

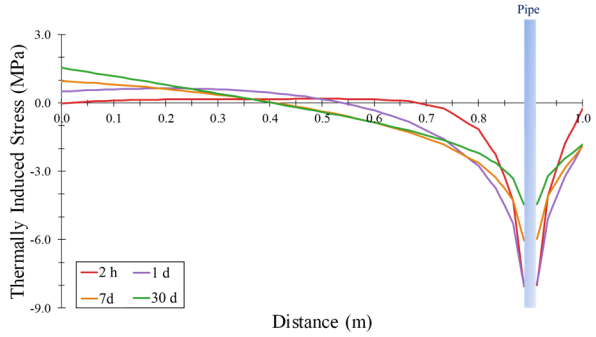

Figure 8. Thermally induced axial stresses at section A for summer scenario.

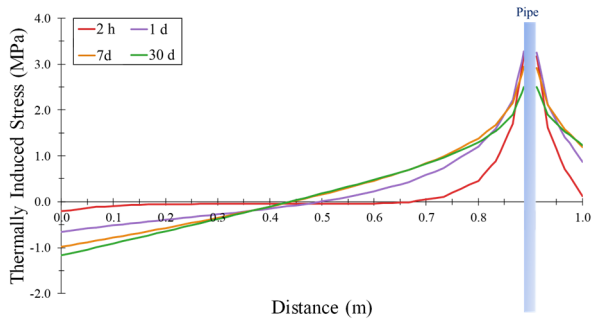

Figure 9. Thermally induced axial stresses at section A for winter scenario.

5 CONCLUSION

This study explored how non-uniform temperature distributions affect the axial stress behavior of energy walls during seasonal heating and cooling operations. Using a validated three-dimensional numerical model, temperature-induced stress responses were simulated under realistic summer and winter conditions, capturing both early and longer-term system behavior.

The findings clearly show that the temperature field within the wall is far from uniform, especially in the early hours of operation, where intense circular gradients develop around the thermal pipes. These localized temperature differences generate significant axial stresses, with compression near the pipes during heating and tension during cooling. Over time, as heat propagates through the wall thickness, a secondary linear gradient form near the building-facing side, further influencing the overall stress distribution.

Importantly, the results reveal that tensile and compressive stresses can occur simultaneously at different parts of the wall, even in the absence of external loads. Some of these tensile stresses may approach critical limits for concrete, especially under repeated thermal cycles. Therefore, understanding the spatial and temporal evolution of thermally induced stresses is essential for the long-term safety and reliability of energy walls.

These insights suggest that simplified or uniform temperature assumptions may not be sufficient in design practice. Instead, detailed consideration of thermal gradients and their mechanical effects is needed to ensure the structural integrity of energy geostructures operating under real environmental conditions.

6 ACKNOWLEDGEMENTS

The authors gratefully acknowledge the support provided by the Scientific and Technological Research Council of Turkey (TÜBİTAK) under the 2224-A grant program.

7 REFERENCES

Abdelaziz, S. and Ozudogru, T.Y. 2016. Non-uniform thermal strains and stresses in energy piles. *Environmental Geotechnics*, 3(4), 237–252.

Bodas Freitas, T.M., Matos Sirgado, R.A., Bourne-Webb, P.J. and de Jesus Silva, D.N. 2024. The influence of geometry on the heat exchange potential of embedded planar retaining walls with seasonally-balanced thermal load. *Applied Thermal Engineering*, 246.

Brandl, H. 2006. Energy foundations and other thermo-active ground structures. *Geotechnique,* 56(2), 81–122.

Erginag, U.C., Guner, M., Polat, S., Sutman, M. and Cinicioglu, O. 2025a. Thermally induced tensile hoop stresses in energy piles: Implications for design and operation. *Geomechanics for Energy and the Environment*, 43.

Erginag, U.C., Guner, M., Polat, S., Sutman, M. and Cinicioglu, O. 2025b.Three-dimensional thermal loads and their effects on the structural performance and durability of energy piles. *In 3rd International Conference on Energy Geotechnics ICEGT2025.*

Faizal, M., Bouazza, A., McCartney, J.S. and Haberfield, C. 2019. Axial and radial thermal responses of energy pile under six storey residential building. *Canadian Geotechnical Journal*, 56(7), 1019–1033.

Laloui, L. and Sutman, M. 2021. Experimental investigation of energy piles: From laboratory to field testing. *Geomechanics for Energy and the Environment*, 27.

Polat, S., Guner, M., Erginag, U.C., Sutman, M. and Cinicioglu, O. 2025a. Analyses of Thermoactive Piles Considering Surface Radiation and Wind Convection Effects. *International Journal of Geomechanics*, 25(1).

Polat, S., Guner, M., Erginag, U.C., Sutman, M. and Cinicioglu, O. 2025b. Incorporating atmospheric and solar influences in numerical analyses of energy piles: A validation study. *In 3rd International Conference on Energy Geotechnics ICEGT2025.*

Sailer, E. 2020. Numerical modelling of thermo-active retaining walls. PhD thesis, Imperial College London.

Sun, M., Xia, C. and Zhang, G. 2013. Heat transfer model and design method for geothermal heat exchange tubes in diaphragm walls. *Energy and Buildings*, 61, 250–259.

Xia, C., Sun, M., Zhang, G., Xiao, S. and Zou, Y. 2012. Experimental study on geothermal heat exchangers buried in diaphragm walls. *Energy and Buildings*, 52, 50–55.